HHS Public Access

Author manuscript

Nat Immunol. Author manuscript; available in PMC 2015 December 01.

Published in final edited form as:

Nat Immunol. 2015 June ; 16(6): 618–627. doi:10.1038/ni.3172.

The ubiquitin-modifying enzyme A20 restricts the ubiquitination of RIPK3 and protects cells from necroptosis

Michio Onizawa[1,*], **Shigeru Oshima**[1,*,@], **Ulf Schulze-Topphoff**[2,*], **Juan A Oses-Prieto**[3], **Timothy Lu**[1], **Rita Tavares**[1], **Thomas Prodhomme**[2], **Bao Duong**[1], **Michael I. Whang**[1], **Rommel Advincula**[1], **Alex Agelidis**[1], **Julio Barrera**[1], **Hao Wu**[4], **Alma Burlingame**[3], **Barbara A. Malynn**[1], **Scott S. Zamvil**[2], and **Averil Ma**[1,#]

[1]Department of Medicine, University of California, San Francisco, San Francisco, CA 94143

[2]Department of Neurology, University of California, San Francisco, San Francisco, CA 94143

[3]Department of Pharmaceutical Chemistry, University of California, San Francisco, San Francisco, CA 94143

[4]Program in Cellular and Molecular Medicine, Boston Children's Hospital, Department of Biological Chemistry and Molecular Pharmacology, Harvard, Medical School, Boston, MA 02115

Abstract

A20 is an anti-inflammatory protein linked to multiple human diseases, however the mechanisms by which A20 prevents inflammatory disease are incompletely defined. We now find that A20 deficient T cells and fibroblasts are susceptible to caspase independent and RIPK3 dependent necroptosis. Global RIPK3 deficiency significantly rescues the survival of A20 deficient mice. A20 deficient cells exhibit exaggerated formation of RIPK1-RIPK3 complexes. RIPK3 undergoes physiological ubiquitination at lysine 5 (K5), and this ubiquitination event supports the formation of RIPK1-RIPK3 complexes. The catalytic cysteine of A20's deubiquitinating motif is required for inhibiting RIPK3 ubiquitination and RIPK1-RIPK3 complex formation. These studies link A20 and RIPK3 ubiquitination to necroptotic cell death, and suggest new mechanisms by which A20 may prevent inflammatory disease.

A20 is a deubiquitinating enzyme that inhibits NF-kB activation and restricts TNF-induced apoptosis[1–4]. A20 is a potent anti-inflammatory protein linked to multiple human autoimmune diseases and to human malignancies[5, 6]. Polymorphisms in the human *TNFAIP3* gene (which encodes the A20 protein) are associated with reduced A20 function or expression that confer susceptibility to autoimmune diseases[7, 8]. Deletion of A20 in mice leads to widespread tissue inflammation and perinatal lethality[2]. A20 regulates multiple signaling cascades and as such, plays distinct physiological functions in different cell types[5, 6]. In myeloid cells, A20 prevents inflammation by restricting the activation of the

[#]To whom correspondence should be addressed: University of California, San Francisco, 513 Parnassus Ave, S-1057, San Francisco, CA 94143-0451. averil.ma@ucsf.edu.

[*]these authors contributed equally

[@]Current address: Department of Gastroenterology and Hepatology, Tokyo Medical and Dental University, Tokyo, Japan

transcription factor NF-κB downstream signals from TLRs, NOD2 and other innate immune receptors[4, 9–14]. These signals lead to the production of pro-inflammatory cytokines such as interleukin 6 (IL-6) and TNF and co-stimulatory molecules that activate other innate immune cells and lymphocytes and lead to autoimmune and inflammatory diseases. In A20-deficient B cells, exaggerated B cell receptor- and CD40-triggered NF-κB activation leads to increased B cell survival and autoimmunity[15–17]. Hence, A20 inhibits NF-κB actvation in various cell types to prevent inflammatory and autoimmune diseases.

The biochemical mechanisms by which A20 restricts signals leading to NF-κB activation are complex and incompletely understood. Ubiquitination of signaling proteins can facilitate their recruitment to non-degradative signaling complexes, often mediated by K63-linked or linear polyubiquitin chains[18]. A20 is an unusual protein that utilizes two distinct motifs to remove activating K63-linked polyubiquitin chains from substrates and build degradative K48-linked ubiquitin chains[3, 4, 19, 20]. A20 may also disrupt E2-E3 ubiquitin ligase interactions by destabilizing E2 enzymes[21]. A20 also possesses ubiquitin binding motifs that support its interaction with RIPK1, E2 and IKKγ[19, 22–25]. In addition, A20 binds E3 ubiquitin ligases such as TRAF2 and TRAF6, ubiquitin sensors, such as ABIN-1 and ABIN-2, and other proteins (e.g., TAX1BP1) that may collaborate with A20 to perform its critical biochemical functions[26]. A20's motifs and protein interactions suggest that A20 regulates multiple signaling cascades by modifying the ubiquitination of key signaling proteins.

Here we have investigated the physiological function of A20 in mouse T cells. We observed decreased expansion of A20-deficient T cells due to exaggerated cell death, and describe a previously unknown function for A20 in protecting T cells against necroptosis, a caspase-independent form of programmed cell death. T cell-specific RIPK3 deficiency restored cell survival in A20-deficient T cells, and global RIPK3 deficiency partially rescued the perinatal lethal phenotype of *Tnfaip3*$^{-/-}$ (called *A20*$^{-/-}$ here) mice. RIPK3 ubiquitination at lysine 5 (K5) of RIPK3 supports RIPK1-RIPK3 complex formation and necroptosis. A20 utilizes its deubiquitinating motif to restrict RIPK3 ubiquitination and the formation of necroptotic RIPK1-RIPK3 complexes.

Results

A20 supports the survival of activated T cells

Tnfaip3$^{fl/fl}$ CD4-Cre mice (called *A20*$^{fl/fl}$ CD4-Cre here) developed normally and survived for at least 6 months without gross disease, suggesting that conditional T cell-specific deletion of A20 does not profoundly perturb cellular immune homeostasis (data not shown). The numbers and frequencies of CD4$^+$CD8$^+$ double positive and CD8$^+$ and CD4$^+$ single positive thymocytes were normal (data not shown). The total numbers of splenic T cells in *A20*$^{fl/fl}$ CD4-Cre mice were similar to those in control *A20*$^{+/fl}$ CD4-Cre mice and *A20*$^{+/+}$ CD4-Cre mice, suggesting that T cell development occurs normally in the absence of A20 (Fig. 1a and data not shown). Analysis of T cell activation markers revealed a greater frequency of T cells with a memory phenotype (CD44^{hi}CD62^{lo} in *A20*$^{fl/fl}$ CD4-Cre mice compared to *A20*$^{+/fl}$ CD4-Cre mice suggesting a role for A20 in regulating T cell responses following antigen exposure (Fig. 1b). Spontaneous T cell activation in *A20*$^{fl/fl}$ CD4-Cre

mice was accompanied by modestly increased myeloid cell (Mac-1^+, $Gr1^+$), but not B cell ($CD19^+$), numbers compared to $A20^{+/fl}$ CD4-Cre mice (Fig. 1a). We observed no difference in all these parameters between $A20^{+/fl}$ CD4-Cre mice and $A20^{+/+}$ CD4-Cre mice, so $A20^{+/fl}$ CD4-Cre mice were used for controls in subsequent experiments.

To investigate the role of A20 in T cell responses, we purified naïve $CD4^+$ T cells from $A20^{fl/fl}$ CD4-Cre and $A20^{+/fl}$ CD4-Cre mice, and stimulated these cells with anti-CD3 and anti-CD28. $A20^{fl/fl}$ CD4-Cre T cells were activated as readily as control cells, as indicated by the expression of CD69 and CD44 activation markers and by expression of IL-2 (data not shown). TCR-stimulated $A20^{fl/fl}$ CD4-Cre T cells diluted CFSE more than control cells (Fig. 1c), indicating that activated A20-deficient $CD4^+$ T cells cycle more than control CD4-Cre T cells. However, the percentage of $A20^{fl/fl}$ CD4-Cre T cells of the total numbers of live T cells on day 2 and 3 after stimulation was markedly lower compared to control cells (Fig. 1d), indicating that A20 deficiency impairs the survival of activated T cells in a cell-autonomous fashion. To normalize potential differences in cytokine production and investigate the cell-autonomous role of A20 in regulating T cell function, we interbred $A20^{fl}$ CD4-Cre mice with CD45.1 congenic mice and stimulated equal (1:1) mixes of sorted naïve congenic $A20^{fl/fl}$ CD4-Cre and control $A20^{+/fl}$ CD4-Cre $CD4^+$ T cells *in vitro*. In these mixed cultures, both A20-deficient and A20-sufficient T cells were exposed to the same amounts of IL-2 and other T cell-derived cytokines. These experiments confirmed that $A20^{fl/fl}$ CD4-Cre T cells expanded poorly compared to $A20^{+/fl}$ CD4-Cre $CD4^+$ T cells (data not shown). To eliminate potential development defects contributed by A20 deficiency and to confirm that A20 directly regulates the survival of mature peripheral T cells, we interbred $A20^{fl/fl}$ mice with ROSA26-ER/Cre mice, which allows the 4-OH-tamixifen inducible deletion of A20. $A20^{fl/fl}$ ROSA26-ER/Cre mice had normal lymphoid populations (data not shown). Sorted naïve $CD4^+$ T cells from $A20^{fl/fl}$ ROSA26-ER/Cre and control $A20^{+/fl}$ ROSA26-ER/Cre mice were mixed and stimulated *in vitro* with anti-CD3 and anti-CD28 antibodies in the presence of 4-OH-tamixifen for three days to induce the efficient deletion of A20 protein (Supplementary Fig. 1). Acute deletion of A20 in $A20^{fl/fl}$ ROSA26-ER/Cre T cells resulted in increased cell death compared to $A20^{+/fl}$ ROSA26-ER/Cre T cells (Fig. 1e), suggesting that A20 directly supports the survival of activated T cells.

Increased RIPK1-RIPK3 complexes in activated A20-deficient T cells

Activated A20-deficient B cells express increased amounts of Bcl-x, which renders them resistant to Fas-mediated death[15]. To investigate how A20 protects survival of activated T cells, we assessed the expression of Bcl-2 family proteins in A20-deficient T cells. Immunoblotting revealed that the expression of Bim, Bax, Bcl-x and Bcl-2 proteins was similar in activated $A20^{fl/fl}$ CD4-Cre and $A20^{+/fl}$ CD4-Cre T cells (Fig. 2a). Increased $A20^{fl/fl}$ CD4-Cre T cell death was also seen after blockade of TNF, Fas or IFN-γ, suggesting cell death in A20-deficient cells is not triggered by these stimuli (Fig. 2b). Importantly, the pan-caspase inhibitors ZVAD or Q-AD did not abrogate the increased cell death in stimulated $A20^{fl/fl}$ CD4-Cre $CD4^+$ T cells, indicating a caspase-independent death pathway (Fig. 2b). Activated T cells die by necroptosis in the absence of the pro-apoptotic proteins FADD or caspase 8[27, 28]. Necroptosis requires RIPK1 kinase activity and the formation of RIPK1-RIPK3 complexes[29–31]. The RIPK1 kinase inhibitor necrostatin 1 (Nec-1)

selectively rescued the survival and expansion of TCR-activated *A20*$^{fl/fl}$ CD4-Cre T cells compared to control cells (Fig. 2b), while an inactive form of Nec-1 was less effective in rescuing *A20*$^{fl/fl}$ CD4-Cre T cell survival (Supplementary Fig. 2). Thus, RIPK1 kinase activity contributes to the increased death of A20-deficient T cells following *in vitro* activation.

Immunoprecipitation of RIPK1 from TCR-activated CD4$^+$ T cells revealed that *A20*$^{fl/fl}$ CD4-Cre T cells contain significantly greater amounts of RIPK1-associated RIPK3 than *A20*$^{+/fl}$ CD4-Cre T cells (Fig. 2c), indicating that RIPK1-RIPK3 complexes accumulate in A20-deficient T cells and suggesting that A20 protects activated T cells from necroptotic death. To further determine the role of RIPK3 in mediating increased cell death in *A20*$^{fl/fl}$ CD4-Cre T cells, we interbred *A20*$^{fl/fl}$ CD4-Cre mice with *Ripk3*$^{-/-}$ mice. Following *in vitro* TCR stimulation for 72 or 120 hours in the presence of ZVAD, the numbers of *A20*$^{fl/fl}$ CD4-Cre *Ripk3*$^{-/-}$ T cells were greater than *A20*$^{fl/fl}$ T cells, though less than control *A20*$^{+/fl}$ T cells (Fig. 2d), indicating that RIPK3 deficiency significantly rescued the survival of activated A20-deficient T cells. The viability of TCR-stimulated caspase 8 deficient Jurkat I9.2 T cells was reduced in cells treated with A20 siRNA relative to control siRNA, and RIPK3 siRNA abrogated the increased cell death observed in A20-deficient Jurkat I9.2 T cells (Fig. 2e), suggesting the epistatic relationship between A20 and RIPK3 is preserved in human cells. Thus, exaggerated death of activated A20-deficient T cells is caspase-independent, is associated with increased RIPK1-RIPK3 complex formation and requires the kinase activity of RIPK1 and the expression of RIPK3.

A20 and RIPK3 control T cell survival during *in vivo* activation

To determine whether A20 regulates T cell survival and responses *in vivo*, we interbred A20^{fl} mice with OT-II TCR transgenic mice. We adoptively co-transferred naive *A20*$^{+/fl}$ CD4-Cre OT-II CD4$^+$ (CD45.1/2) T cells and *A20*$^{fl/fl}$ CD4-Cre OT-II CD4$^+$ (CD45.1) T cells into C57BL/6 (CD45.2) recipients, immunized these mice with LPS plus ovalbumin peptide (OVA) 24 h after transfer (day 0) and quantitated the numbers of splenic OT-II T cells from both donor genotypes at various time points after immunization. This experimental design allowed us to assess the response of A20-deficient and A20-sufficient T cells in the same cytokine and environmental factors milieu. Consistent with the *in vitro* data, *A20*$^{fl/fl}$ CD4-Cre OT-II CD4$^+$ T cells expanded poorly relative to control CD4-Cre OT-II CD4$^+$ T cells 3 and 7 days activated within the same miceafter OVA challenge (Fig. 3a). This result indicates that A20 supports expansion of activated T cells *in vivo*.

We next tested the susceptibility of *A20*$^{fl/fl}$ CD4-Cre mice to experimental autoimmune encephalomyelitis (EAE), a model of T cell-mediated autoimmunity[32]. Following immunization with a myelin oligodendrocyte glycoprotein (MOG) peptide in Freund's complete adjuvant, *A20*$^{fl/fl}$ CD4-Cre mice developed markedly less severe motor neuron symptoms than control *A20*$^{+/fl}$ CD4-Cre mice (Fig. 3b). Histological studies revealed fewer lymphoid infiltrates and greater myelin preservation in spinal cord sections from *A20*$^{fl/fl}$ CD4-Cre mice than control mice (Fig. 3c), while *ex vivo* MOG stimulation of lymph node CD4$^+$ T cells showed decreased proliferation of *A20*$^{fl/fl}$ CD4-Cre T cells *in vitro* compared to *A20*$^{+/fl}$ CD4-Cre T cells (Fig. 3d). T_H17 cells are important in the pathogenesis of EAE[33].

We thus quantitated the number of T_H17 cells from the lymph nodes of MOG-immunized mice and found fewer T_H17 cells in the *A20*$^{fl/fl}$ CD4-Cre lymph nodes compared to A20$^{+/fl}$ CD4-Cre controls (Fig. 3e), which paralleled the reduction of MOG-specific A20-deficient CD4$^+$ T cells (Fig. 3d). Following the *in vitro* stimulation of naïve CD4$^+$ T cells under T_H1 or T_H17 polarizing conditions, fewer IFN-γ-producing and IL-17-producing T cells were obtained from *A20*$^{fl/fl}$ CD4-Cre T cell cultures compared to control *A20*$^{+/fl}$ CD4-Cre cultures (Supplementary Fig. 3), while T_H17 and T_H1 differentiation from *A20*$^{fl/fl}$ CD4-Cre *Ripk3*$^{-/-}$ T cells was equal to that from *A20*$^{+/fl}$ CD4-Cre T cells and *A20*$^{+/fl}$ CD4-Cre *Ripk3*$^{-/-}$ T cells (Supplementary Fig. 3). Hence, T cell-specific A20 deficiency impairs T cell activation and CD4$^+$ T cell differentiation into T_H17 and T_H1 cells and renders mice less susceptible to EAE.

We next examined if RIPK3-dependent necroptosis affected the survival of A20-deficient T cells *in vivo*. RIPK3 is expressed in multiple tissues, and *Ripk3*$^{fl/fl}$ mice have not yet been described. Hence, we adoptively transferred CD4$^+$ T cells from *A20*$^{fl/fl}$ CD4-Cre *Ripk3*$^{-/-}$ or *A20*$^{fl/fl}$ CD4-Cre *Ripk3*$^{+/+}$ control mice into *Rag1*$^{-/-}$ hosts, which were subsequently immunized with MOG peptide. This experimental design allowed interrogation of the T cell-specific function of A20 and RIPK3 *in vivo*. *Rag1*$^{-/-}$ mice that received *A20*$^{fl/fl}$ CD4-Cre *Ripk3*$^{-/-}$ T cells developed more severe EAE than RAG-1$^{-/-}$ mice that received *A20*$^{fl/fl}$ CD4-Cre *Ripk3*$^{+/+}$ T cells (Fig. 3f). Taken together, these data indicate that A20 protects activated CD4$^+$ T cells from RIPK3-dependent necroptosis *in vivo*.

A20 protects mice from RIPK3-dependent necroptosis

Necroptotic death typically triggers inflammation *in vivo* due to the release of intracellular molecules from dying cells[34]. Tissue death and inflammation are hallmarks of *A20*$^{-/-}$ mice[2]. To test if A20 might prevent necroptosis in cells other than T cells, we derived mice bearing germline deletion of the floxed A20 exon 2 by interbreeding *A20*$^{fl/fl}$ mice with B6.EIIA-Cre mice (which deletes floxed alleles in the early mouse embryo)[15]. Mice bearing germline deletion of A20 exon 2, defined as *A20*^{ko2} mice, were bred to C57BL/6 mice to generate A20^{ko2} mice that lacked the EIIA-Cre transgene. *A20*^{ko2} mice were subsequently crossed with *Ripk3*$^{-/-}$ mice to generate *A20*$^{ko2/ko2}$ *Ripk3*$^{-/-}$ double mutant mice (in the C57BL/6 background). While most *A20*$^{ko2/ko2}$ *Ripk3*$^{+/+}$ mice died within 1 day of birth, *A20*$^{ko2/ko2}$ *Ripk3*$^{-/-}$ mice survived 2–3 weeks before succumbing to inflammatory death (Fig. 4a). The partial rescue of *A20*$^{ko2/ko2}$ mice lethality by RIPK3 deficiency suggests that increased systemic necroptosis contributes to the perinatal lethality observed in *A20*$^{ko2/ko2}$ mice.

Because increased T cells necroptosis is unlikely to be the main cause of the perinatal lethality in *A20*$^{ko2/ko2}$ mice, we next tested whether A20 directly restricts necroptosis in non-T cells. We isolated mouse embryonic fibroblasts (MEFs) from *A20*$^{ko2/ko2}$ and *A20*$^{+/+}$ mice, and tested their susceptibility to cell death in response to TNF, cycloheximide (CHX) and ZVAD, a cocktail known to induce caspase-independent necroptosis. In these conditions, as assessed using CellTiter-Glo luminescence, more *A20*$^{ko2/ko2}$ MEFs died compared to wild-type MEFs (Fig. 4b). Treatment of TNF, CHX, ZVAD-stimulated MEFs with Nec-1 rescued the viability of *A20*$^{ko2/ko2}$ MEFs to that of wild-type MEFs (Fig. 4b), suggesting that the caspase-independent death induced by the TNF-CHX-ZVAD mix was

RIPK1 kinase activity-dependent. *A20*$^{ko2/ko2}$ *Ripk3*$^{-/-}$ MEFs were protected from TNF-CHX-ZVAD-induced necroptosis when compared to *A20*$^{ko2/ko2}$ MEFs, indicating that A20 inhibits RIPK3-dependent necroptosis in these cells (Fig. 4b). Taken together, these results indicate that A20 protects multiple cell types from necroptosis, and suggests that uncontrolled necroptosis contributes to the perinatally lethal phenotype of *A20*$^{ko2/ko2}$ mice.

A20 inhibits pro-necroptotic RIPK1-RIPK3 complexes

RIPK3-dependent necroptosis involves RIPK1 kinase and RIPK3 dependent formation of RIPK1-RIPK3 complexes[29, 30]. Accordingly, we tested whether A20 restricted the formation of RIPK1-RIPK3 complexes in a cell autonomous fashion. We immunoprecipitated RIPK1 from WT and *A20*$^{ko2/ko2}$ MEFS treated with either TNF-CHX or TNF-CHX-ZVAD and immunoblotted for RIPK3. Treatment with TNF-CHX- ZVAD induced higher amounts of RIPK1-associated RIPK3 in *A20*$^{ko2/ko2}$ MEFs compared to *A20*$^{+/+}$ MEFs (Fig. 4c). Because phosphorylation of RIPK3 is required for the formation of necroptotic RIPK1-RIPK3 complexes, we tested the phosphorylation status of RIPK3 in *A20*$^{ko2/ko2}$ MEFs[29, 30]. We stimulated *A20*$^{ko2/ko2}$ MEFs with TNF-CHX-ZVAD, immunoprecipitated RIPK1, and then treated these RIPK1 immunoprecipitates with lambda phosphatase (or buffer control). Immunoblot analyses of RIPK3 expression in these samples revealed that RIPK1-associated RIPK3 was phosphorylated (Fig. 4d), suggesting that A20 inhibits the formation of pro-necroptotic RIPK1-RIPK3 complexes that contain phosphorylated RIPK3.

RIPK3 ubiquitination supports RIPK1-RIPK3 complexes and necroptosis

The laddered species at ~8kd intervals detected with an anti-RIPK3 antibody in the RIPK1 immunoprecipitates suggests that the RIPK3 proteins, rather than non-covalently associated co-precipitated proteins, are modified (Fig. 4c, d). To more precisely define RIPK3 ubiquitination, we used anti-gly-gly antibody assisted mass spectrometry (termed “ubiscan”) to search for ubiquitinated RIPK3 peptides in necroptotic MEFs[35]. We stimulated *A20*$^{ko2/ko2}$ MEFs with TNF-CHX-ZVAD, trypsinized whole cell protein lysates, immunoprecipitated the tryptic lysates with an antibody directed against gly-gly remnants of ubiquitinated lysines and performed mass spectrometric analyses of the affinity-purified ubiquitinated peptides. Tandem mass spectra from *A20*$^{ko2/ko2}$ MEF lysates repeatedly revealed a precursor ion with an m/z value of 1006.0525^{+2} (Fig. 5a). A data base search identified this species as a peptide spanning the amino acids 2 to 19 of RIPK3, which was acetylated at the N-terminus and carried a di-glycine remnant at the lysine 5 (K5) residue (theoretical monoisotopic m/z= 1006.0522^{+2}). Because this modification was observed in endogenous proteins from TNF-CHX-ZVAD-stimulated *A20*$^{ko2/ko2}$ MEFs, these observations indicate that RIPK3 ubiquitination at position K5 is a physiological modification.

To quantify if RIPK3 ubiquitination at position K5 is dependent upon A20, we performed stable isotope labeling (SILAC) of *A20*$^{ko2/ko2}$ and wild-type MEFs[35]. *A20*$^{ko2/ko2}$ MEFs were grown in “light” (normal) isotope labeled media and wild-type MEFs were grown in “heavy” isotope labeled media for two weeks. Complete replacement of endogenous amino acids by isotope labeled residues was confirmed by mass spectrometry (data not shown). Labeled MEFs were stimulated with TNF-CHX-ZVAD for three hours, lysates from

A20$^{ko2/ko2}$ and wild-type MEFs were mixed, trypsinized and immunoprecipitated for ubiquitinated peptides prior to LC-MS mass spectrometric analysis. Tandem mass spectra revealed species with m/z ~ 1006, indicating the presence of RIPK3 peptide ubiquitinated at position K5 in normal ("light")-labeled A20$^{ko2/ko2}$ MEFs (Fig. 5b). These spectra also revealed species at m/z ~1015, indicative of RIPK3 peptide modified at position K5 with "heavy" isotope labeled residues in wild-type MEF cells (Fig. 5b, left). Direct comparison of the relative intensity of these peaks showed that m/z~1006 species were ~15-fold more abundant than m/z~1015 species, thereby indicating that *A20*$^{ko2/ko2}$ MEF cells contained 15-fold greater amounts of K5-ubiquitinated RIPK3 peptide than wild-type MEF cells (Fig. 5b, **right**). As *A20*$^{ko2/ko2}$ MEFs express similar amounts of total RIPK3 protein as wild-type MEF cells (Fig. 4c), these findings indicate increased RIPK3 ubiquitination at position K5 in A20-deficient cells. K5-ubiquitinated RIPK3 peptides were not detected in lysates from unstimulated *A20*^{ko2ko2} or control MEFs (data not shown), supporting the notion that ubiquitination at position K5 of RIPK3 is induced during necroptosis.

To determine the functional importance of RIPK3 ubiquitination at position K5 in necroptosis, we mutated K5 to alanine (K5A) or arginine (K5R). Because the K5R RIPK3 mutant was not stable (data not shown), we tested the ability of K5A RIPK3 to form RIPK1-RIPK3 complexes in necroptotic cells. We virally transduced wild-type or K5A RIPK3 into *A20*$^{ko2/ko2}$ *Ripk3*$^{-/-}$ MEFs, sorted transduced cells expressing similar amounts of RIPK3 and analyzed the amount of RIPK1-associated RIPK3 expression as well as the amount of cellular necroptosis following TNF-CHX-ZVAD stimulation. MEFs expressing the K5A RIPK3 exhibited decreased RIPK1-RIPK3 complexes when compared to cells expressing wild-type RIPK3 (Fig. 5c). Furthermore, cells expressing K5A RIPK3 survived significantly better than cells expressing wild-type RIPK3 (Fig. 5d), indicating that ubiquitination of RIPK3 at position K5 supports the formation of RIPK1-RIPK3 complexes and necroptosis.

A20 utilizes its deubiquitinating motif to restrict necroptosis

Polyubiquitin chains of various conformations are added to target proteins during cell signaling[18]. Because A20 restricts RIPK1 ubiquitination with K63-linked polyubiquitin chains, we investigated whether A20 also inhibits RIPK3 ubiquitination with K63-linked polyubiquitin chains. 293T cells were transfected with plasmids expressing RIPK3, and HA-K63-Ub (ubiquitin in which all ubiquitin lysines except K63 are mutated). Lysates were immunoprecipitated with anti-RIPK3 and immunoblotted with anti-HA to reveal a ladder of K63-ubiqitinated RIPK3 (Fig. 6a). Addition of increasing amounts of Flag-A20 plasmid to the transfection led to a progressive decrease in the amount of HA-K63-Ub signal (Fig. 6a), indicating that A20 inhibited the K63-linked ubiquitination of RIPK3 in a dose-dependent fashion. In addition, increased K63-linked ubiquitination of RIPK3 was found in *A20*$^{ko2/ko2}$ MEFs compared to wild-type MEFs following stimulation with TNF-CHX-ZVAD (Fig. 6b). Thus, A20 restricts K63-linked ubiquitination of RIPK3.

To determine the mechanism by which A20 restricts RIPK3 ubiquitination, we used MEFs from two lines of knockin mice bearing point mutations that abrogate the enzymatic activity of each domain. *A20*^{OTU} mice bear a mutation in the catalytic cysteine 103 (C103) residue of A20 that mediates A20's deubiquitinating activity[19]. *A20*^{ZF4} mice bear point mutations

(C609, C612) in the ZF4 domain that mediates A20's binding to ubiquitinated RIP1[19]. *A20*$^{ZF4/ZF4}$ or wild-type MEFs showed comparable viability in response to TNF-CHX-ZVAD, whereas *A20*$^{OTU/OTU}$ MEFs had reduced viability (Fig. 6c), indicating that A20 uses its catalytic deubiquitinating Cys103 residue to inhibit necroptosis.

To understand how A20's C103 and ZF4 motifs regulate necroptotic signaling complexes, we analyzed the formation of RIPK1-RIPK3 complexes in *A20*^{ZF4ZF4} and *A20*^{OTUOTU} MEFs. After stimulation of wild-type, *A20*^{ZF4ZF4} and *A20*^{OTUOTU} MEFs with TNF-CHX-ZVAD for 3 or 4 hours, protein lysates were immunoprecipitated with anti-RIPK1 and immunoblotted with anti-RIPK3. *A20*$^{OTU/OTU}$ MEFs contained markedly increased RIPK1-RIPK3 complexes when compared to wild-type or *A20*$^{ZF4/ZF4}$ MEFs (Fig. 6d), while *A20*$^{ZF4/ZF4}$ MEF cells contained modestly elevated RIPK1-RIPK3 complexes when compared to wild-type MEFs (Fig. 6d). RIPK1-associated RIPK3 showed a laddered pattern indicative of ubiquitination in *A20*$^{OTU/OTU}$ MEFs (Fig. 6d). *A20*$^{OTU/-}$ T cells also exhibited greater amounts of RIPK1-RIPK3 association and greater RIPK3 ubiquitination than either *A20*$^{ZF4/-}$ or *A20*$^{+/-}$ T cells following TCR stimulation (Fig. 6e), indicating that Cys103 regulates RIPK3 ubiquitination and RIPK1-RIPK3 complex formation in T cells as well as in MEFs. In addition, *A20*$^{OTU/-}$ T cells and *A20*$^{ZF4/-}$ survival was decreased compared to *A20*$^{+/-}$ T cells following 72 hours of stimulation with anti-CD3, anti-CD28, and ZVAD for 72 hours (Fig. 6f). TCR-ZVAD stimulated *A20*$^{OTU/OTU}$ and *A20*$^{ZF4/ZF4}$ T cells exhibited similar relative phenotypes as *A20*$^{OTU/-}$ T cells and *A20*$^{ZF4/-}$ T cells (data not shown). Finally, *A20*^{OTU} and A20^{ZF4} mice were crossed with *Ripk3*$^{-/-}$ mice and the responses to TCR-ZVAD stimulation in naïve CD4^{+} T cells isolated from these mice were tested. Following TCR-ZVAD stimulation for 72 hours, expansion of *A20*$^{OTU/-}$ *Ripk3*$^{-/-}$ CD4^{+} T cells was the same as *A20*$^{+/-}$ T cells, and expansion of *A20*$^{ZF4/-}$ *Ripk3*$^{-/-}$ CD4^{+} T cells was partially restored to that of *A20*$^{+/-}$ T cells (Fig. 6f), indicating that RIPK3-deficiency restored expansion of TCR-ZVAD stimulated *A20*$^{OTU/-}$, and to a lesser extent, *A20*$^{ZF4/-}$ CD4^{+} T cells. This indicates that while the ZF4 domain of A20 is also required for normal A20 activity during T cell activation, the Cys103-dependent deubiquitination function of A20 is required to inhibit the formation of RIPK1-RIPK3 complexes and RIPK3-dependent necroptosis.

Discussion

Our study reveals that A20 restricts necroptosis in multiple cell types. These findings suggest A20 regulates cellular and tissue homeostasis as well as immune homeostasis. We have discovered that RIPK3 undergoes a specific ubiquitination event that supports the formation of RIPK1-RIPK3 complexes in cells undergoing necroptosis, and that A20 potently inhibits this event. Our studies have broad implications for the molecular regulation of cell death signaling as well as the physiological mechanisms by which A20 prevents inflammatory diseases.

We have found that uncontrolled RIPK3-dependent necroptosis in the absence of A20 inhibited T cell expansion *in vitro* and *in vivo*. Exaggerated necroptosis in caspase-8 deficient and FADD mutant T cells has been reported to compromise anti-LCMV or anti-Toxoplasma responses[27, 28]. Hence, our studies reinforce the concept that, in certain

pathological contexts, necroptosis can restrict the expansion of activated T cells. Our studies also indicate that A20 has dual roles in T cells, restricting both cellular activation and cell death. Activation and survival signals appear to be integrated differently in activated T cells compared to activated B cells, in which A20 deficiency causes increased NF-κB-dependent Bcl-x expression and resistance to Fas-mediated death[13]. These differences re-emphasize the importance of studying the cell type-specific functions of pleiotropically expressed molecules to understand their physiological roles in disease pathogenesis.

Our finding that $A20^{KO2/KO2}$ $RIPK3^{-/-}$ mice live longer than $A20^{KO2/KO2}$ mice suggested that A20 protects multiple cell types from necroptosis. As such, loss of A20 from other cells (e.g., stromal cells) may render mice more susceptible to necroptotic tissue damage. Our observations are consistent with prior experiments showing that A20 protects L929 fibrosarcoma cells from TNF-induced death[36]. RIPK3 deficiency might also abrogate inflammasome activity in $A20^{-/-}$ mice[37]. Because A20 also protects cells against apoptotic death[2, 38], the anti-necroptotic function of A20 positions this molecule as a potent pro-survival protein. The notion that necroptosis of target organs may contribute to disease severity has been suggested in inflammatory bowel disease and other conditions[39]. Considered together with observations that A20 polymorphisms are associated with more severe nephritic complications of SLE patients and increased disease severity in psoriasis vulgaris and cystic fibrosis patients, A20 may partly prevent human disease by protecting against necroptotic death in non-lymphoid tissues[40–42].

Necroptosis is known to occur in cells lacking pro-apoptotic molecules such as caspase 8 and FADD[43–46]. This has been explained by the cleavage of RIPK1 by caspase 8, which prevents RIPK1 kinase-dependent formation of RIPK1-RIPK3 complexes. Virally infected cells may also undergo necroptosis when viral proteins abrogate apoptosis[30]. Hence, necroptosis has been viewed as a form of cell death that occurs predominantly in cells rendered caspase deficient. By contrast, we have found that A20-deficient MEFs exhibit increased sensitivity to both apoptosis and necroptosis[2]. Therefore, our findings suggest that A20 restricts necroptosis in a fashion that is distinct from caspase 8 or FADD.

RIPK1 ubiquitination inhibits RIPK1 kinase activity, and the deubiquitinating enzyme CylD supports necroptosis by deubiquitinating RIP1[46, 47]. Like CylD, A20 inhibits RIPK1 ubiquitination and NF-κB signaling[3, 19]. However, unlike CylD, our current findings show that A20 inhibits necroptosis. This divergence suggests that A20 inhibits necroptosis via a mechanism other than inhibiting RIPK1 ubiquitination. Our finding that A20 restricted RIPK3 ubiquitination provide such a mechanism. K63-linked ubiquitination of RIPK1 and RIP2 occur during TNF- and NOD2-induced NF-κB signaling, respectively, and *$A20^{-/-}$* MEFs and macrophages exhibit increased RIPK1 and RIP2 ubiquitination, respectively when stimulated through these pathways[3, 10, 19]. Hence, A20 appears to restrict RIPK1, RIP2 and RIPK3 ubiquitination in distinct signaling contexts. The cIAP E3 ligases can ubiquitinate RIP family proteins *in vitro*, and cIAP1 and cIAP2 may be responsible for activating RIPK1 and RIP2 by supporting their ubiquitination with K63-linked chains following TNF and NOD2 pathway activation[48, 49]. Hence, one might speculate that cIAPs similarly activate RIPK3 through ubiquitination during necroptosis. However, cIAPs appear to limit necroptosis in macrophages[48]. Thus, if cIAPs activate RIPK3 and support RIPK1-

RIPK3 complex formation and necroptosis, they likely also perform a separate function that restricts necroptosis (e.g., cIAPs could ubiquitinate RIPK1). Future studies will be needed to identify the physiological E3 ligases that ubiquitinate RIPK3.

Our mass spectrometric screen identified K5 of RIPK3 as a physiological ubiquitination site, and our SILAC experiments revealed that A20$^{-/-}$ MEFs contain 15-fold more RIPK3 peptide ubiquitinated at K5 than wild-type MEFs. Mutation of this residue abrogated RIPK3 ubiquitination and the formation of RIPK1-RIPK3 complexes and necroptosis. In other signaling complexes, K63-linked ubiquitination facilitates the recruitment of K63-ubiquitin sensor proteins[18]. Hence, K63-linked ubiquitination of RIPK3 could similarly support the recruitment of other ubiquitin sensors. These ubiquitin binding proteins could in turn enhance RIPK3 kinase activity, support RIPK1-RIPK3 complexes, recruit downstream mediators such as MLKL[51], and/or support higher-order amyloid complexes comprised of RIPK1 and RIPK3 proteins[31]. Structurally, K5 resides in an unstructured portion of RIPK3, and is thus likely to be accessible for ubiquitination[52]. In addition, the K5 residue is conserved in human RIPK3, and RIPK3 deficiency abrogated increased necroptosis of A20-deficient human Jurkat I9.2 T cells. Thus, RIPK3 ubiquitination may support necroptosis in human cells. Therefore, ubiquitination can support necroptosis, and A20 strongly inhibits this pro-necroptotic ubiquitination event.

We have found that A20's C103 deubiquitinating motif was required for inhibiting RIPK3 ubiquitination and forming RIPK1-RIPK3 complexes. The C103 motif cleaves unanchored K48 ubiquitin chains as well as RIPK1- or TRAF6- anchored K63 chains in cell-free experiments[3, 4, 20]. This motif has also been shown to inhibit E2-E3 interactions in cells[21]. Both these C103-dependent activities could inhibit the K63-linked polyubiquitination of RIPK3. In contrast, A20's ZF4, which binds ubiquitin and supports E3 ligase activity, appeared less critical than C103 for inhibiting RIPK3 ubiquitination during necroptosis. One possible explanation for this difference could be that A20, which relies upon ZF4 to bind ubiquitinated RIPK1, may rely more on other ubiquitin binding motifs, such as ZF7, to bind ubiquitinated RIPK3. Such distinct roles for A20's biochemical motifs can provide important insights into how A20 performs its physiological functions.

In conclusion, we have discovered that A20 restricts RIPK3 dependent necroptosis. Our studies show that RIPK3 is physiologically ubiquitinated at K5 during necroptosis in a manner that supports the formation of RIPK1-RIPK3 complexes. A20's regulation of necroptosis should be integrated with A20's previously described roles in restricting NFkB signaling and cellular activation. As hypomorphic A20 expression and function are linked to a wide range of human inflammatory and autoimmune diseases, and as necroptosis can trigger inflammation, our studies suggest a new pathway by which A20 prevents human disease.

Online Methods

Mice and in vivo experiments

The generation of mice bearing a "floxed" allele of A20 (*A20*^{fl} mice) has been described (9, 13). Mice lacking A20 specifically in T cells were generated by breeding *A20*^{fl} mice with

CD4-Cre transgenic mice. Mice bearing gene-targeted point mutations in the A20 gene, *A20*^{OTU} mice and *A20*^{ZF4} mice, were recently described[19]. *Ripk3*$^{-/-}$ mice were kindly provided by X. Wang. *A20*$^{-/-}$ mice were generated by breeding *A20*^{fl} mice with B6.EIIA-Cre mice, and subsequently breeding to C57BL/6J mice and selecting for mice bearing the predicted A20 exon 2 deletion but not the EIIA-Cre transgene. *RAG1*$^{-/-}$ mice were purchased from Jackson Labs. All mice were generated and maintained on a C57BL/6 inbred background, and all mouse experiments were performed according to UCSF institutional guidelines.

For antigen specific T cell responses, naïve TCR transgenic OT-II CD4^{+} T cells were flow cytometrically purified from congenically marked mice, mixed 1:1, CFSE labeled, and adoptively transferred into C57BL/6J mice. Mice were immunized with OVAp (200 mg) and LPS (20ug) 24 hours after cell transfer, and analyzed at various time points. For EAE experiments, mice were immunized with MOG peptide p35–55 (50 μg) in CFA with pertussis toxin (200 ng). Clinical symptoms and histological analyses were performed as previously described[53].

In vitro T cell analysis

For in vitro T cell assays, naïve (CD4^{+} CD25^{-} CD44^{Lo} CD62L^{Hi}) T cells were purified by bead enrichment and/or flow cytometric sorting from spleens and lymph nodes from the indicated strains of mice prior to stimulation with plate bound anti-CD3 (2.5 μg/ml; UCSF Monoclonal Antibody Core) and anti-CD28 (2 μg/ml; UCSF Monoclonal Antibody Core). In addition, mIL-12 (20ng/ml, Peprotech) and anti-IL-4 (10μg/ml, 11B11:Tonbo) were used for T_H1 polarization, while hTGFβ (5ng/ml, Peprotech), mIL-6 (20ng/ml, Peprotech), anti-IL-4 (10μg/ml) and anti-IFNγ (10μg/ml, XMG1.2, UCSF hybridoma core) were used for T_H17 polarization. In selected experiments, T cells were labeled with 3 mM CFSE (Invitrogen). siRNA mediated reduction of RIPK3 in Jurkat I9.2 cells (ATCC) was performed using one pulse of 2200 V and 20 ms, using Neon Transfection System (Invitrogen) according to manufacturer's instructions.

Flow Cytometry

Cell survival of MEFs was quantitated using the CellTiter-Glo Luminescent Cell Viability Assay per manufacturer's instructions (Promega). The following antibodies were purchased (BD bioscience) and used for FACS studies: anti-CD4-PEcy7, anti-CD4-APC, anti-CD8-PEcy7, anti-CD8-APC, anti-CD11b–PEcy7, anti-Gr1-APC, anti-CD45.1-APC, anti-CD45.1-FITC, anti-CD45.2-APC, anti-CD45.2-FITC, anti-CD44-FITC, anti-CD62L–PE, anti-CD62L–APC, anti-TCRβ-FITC. Live cells were quantitated by flow cytometry of DAPI-negative cells. For intracellular cytokine expression, cells were incubated with PMA (50 ng/ml, Sigma-Aldrich), ionomycin (250 ng/ml, Sigma-Aldrich) and GolgiPlug (1 μl/ml, BD Bioscience) for 4 hrs before harvesting. Cells were stained using anti-CD4-e450 (Tonbo), anti-IFNγ−PE (BD Bioscience), anti-IL17A–Alexa647 (BD Bioscience), Live/Dead cell stain kit (Invitrogen) and Cytofix/Cytoperm kit (BD Bioscience).

Signaling assays

Stimulated T cells were incubated in lysis buffer. For signaling complex analyses, cell lysates were pre-cleared with Protein G beads prior to immunoprecipitation with anti-RIPK1 antibody. Antibodies and reagents used for immunoprecipitation and immunoblotting studies included: anti-RIPK1, anti-Bim, anti-Bclx, (BD Biosciences), nec1, anti-Bcl2, β-actin (Merck chemicals), anti-RIPK3 (ProSci Incorporated), anti-ubiquitin, anti-Bax, anti-RIPK3 (Santa Cruz Biotechnology), anti-RIPK1, anti-A20 (Cell signaling Technology), QVD, ZVAD (Enzo Life Science).

Signaling studies in MEFs were performed as described[19]. RIPK1 immunoprecipitations were performed using anti-RIPK1 (Cell Signaling) and Dynabeads M270 Epoxy (Invitrogen). K63-ubiquitin immunoprecipitations were performed using anti-K63 (Millipore) and Dynabead Protein A (Invitrogen). Studies of RIPK3 mutants in *A20*$^{-/-}$ *Ripk3*$^{-/-}$ MEFs were performed by generating RIPK3 lysine mutants, introducing mutant RIPK3-encoding cDNAs into GFP expressing lentiviral constructs, and infecting *A20*$^{-/-}$ *Ripk3*$^{-/-}$ MEFs with these viruses. Productively infected cells were FACS-sorted to obtain pure populations of RIPK3-expressing cells prior to being tested in necroptosis assays. Cell survival of MEFs was quantitated using the CellTiter-Glo Luminescent Cell Viability Assay per manufacturer's instructions (Promega).

Mass spectrometry

Pellets of stimulated cells were solubilized in urea, ammonium bicarbonate and TCEP, alkylated with iodoacetic acid, and digested overnight with TPCK modified trypsin. Tryptic peptides were enriched for ubiquitinated peptides with the PTMScan Ubiquitin Remnant Motif kit (Cell Signaling Technology) according to the manufacturer's protocol. Affinity purified ubiquitinated peptides were separated by nano-flow liquid chromatography, the eluate coupled to a ion trap-Orbitrap mass spectrometer, and peptides analyzed using PAVA in-house software. For quantitative (SILAC) mass spectrometry experiments, ko2 and A20$^{+/+}$ MEFs were passaged in the presence of dialyzed serum supplemented with either heavy (*A20*$^{+/+}$) or light (*A20*$^{ko2/ko2}$) isotope labeled amino acids for two weeks prior to stimulation. Lysates from *A20*$^{+/+}$ and *A20*$^{ko2/ko2}$ cells were mixed, trypsinized and immunoprecipitated with anti-gly-gly (ubiscan) prior to mass spectrometry analysis[35].

Supplementary Material

Refer to Web version on PubMed Central for supplementary material.

Acknowledgements

This work was supported by the NIH (DK071939 and DK095693 [A.M.]; AI073737 and NS063008 [S.S.Z.]), the Kenneth Rainin Foundation (A.M.), the NMSS (RG 4768 and RG 5180 [S.S.Z.]), the Guthy Jackson Charitable Foundation and Maisin Foundation (S.S.Z.). M.O. and S.O. were partially supported by the CCFA; U.S. was supported by the NMSS. We thank Juan Carlos Patarroyo and Nicolas Molnarfi for assistance with EAE experiments. We thank Scott Oakes for helpful discussions. Mass spectrometry analysis was provided by the Bio-Organic Biomedical Mass Spectrometry Resource at UCSF (A.L. Burlingame, Director) supported by funding from the Biomedical Technology Research Centers program of the NIH National Institute of General Medical Sciences, NIH NIGMS 8P41GM103481 and Howard Hughes Medical Institute.

References

1. Opipari AW Jr, Boguski MS, Dixit VM. The A20 cDNA induced by tumor necrosis factor alpha encodes a novel type of zinc finger protein. J. Biol. Chem. 1990; 265:14705–14708. [PubMed: 2118515]
2. Lee EG, et al. Failure to regulate TNF-induced NF-kappaB and cell death responses in A20-deficient mice. Science. 2000; 289:2350–2354. [PubMed: 11009421]
3. Wertz IE, et al. De-ubiquitination and ubiquitin ligase domains of A20 downregulate NF-κB signalling. Nature. 2004; 430:694–699. [PubMed: 15258597]
4. Boone DL, et al. The ubiquitin modifiying enzyme A20 is essential for terminating TLR signaling. Nat. Immunol. 2004; 5:1052–1060. [PubMed: 15334086]
5. Ma A, Malynn BA. A20: Linking ubiquitination with immunity and human diseases. Nat. Rev. Immunol. 2012; 12:774–785. [PubMed: 23059429]
6. Catrysse L, Vereecke L, Beyaert R, van Loo G. A20 in inflammation and autoimmunity. Trends in Immunol. 2014; 35:22–31. [PubMed: 24246475]
7. Musone S, et al. Multiple polymorphisms in the TNFAIP3 region are independently associated with systemic lupus erythematosus. Nat. Genet. 2008; 40:1062–1064. [PubMed: 19165919]
8. Adrianto I, et al. Association of a functional variant downstream of TNFAIP3 with systemic lupus erythematosus. Nat. Genet. 2011; 43:253–258. [PubMed: 21336280]
9. Turer EE, et al. Homeostatic MyD88-dependent signals cause lethal inflammation in the absence of A20. J. Exp. Med. 2008; 205:451–464. [PubMed: 18268035]
10. Hitotsumatsu O, et al. The ubiquitin-editing enzyme A20 restricts nucleotide-binding oligomerization domain containing 2-triggered signals. Immunity. 2008; 28:381–390. [PubMed: 18342009]
11. Kool M, et al. The ubiquitin-editing protein A20 prevents dendritic cell activation, recognition of apoptotic cells, and systemic autoimmunity. Immunity. 2011; 35:82–96. [PubMed: 21723156]
12. Hammer GE, et al. Expression of A20 by dendritic cells preserves immune homeostasis and prevents colitis and spondyloarthritis. Nat. Immunol. 2011; 12:1184–1193. [PubMed: 22019834]
13. Matmati M, et al. A20 (TNFAIP3) deficiency in myeloid cells triggers erosive polyarthritis resembling rheumatoid arthritis. Nat. Genet. 2011; 43:908–912. [PubMed: 21841782]
14. Heger K, et al. A20 deficient mast cells exacerbate inflammatory responses in vivo. PLoS Biol. 2014; 12:e1001762. [PubMed: 24453940]
15. Tavares RM, et al. The ubiquitin modifying enzyme A20 restricts B cell survival and prevents autoimmunity. Immunity. 2010; 33:181–191. [PubMed: 20705491]
16. Chu Y, et al. B cells lacking the tumor suppressor TNFAIP3/A20 display impaired differentiation and hyperactivation and cause inflammation and autoimmunity in aged mice. Blood. 2011; 117:2227–2236. [PubMed: 21088135]
17. Hövelmeyer N, et al. A20 deficiency in B cells enhances B-cell proliferation and results in the development of autoantibodies. Eur. J. Immunol. 2011; 41:595–601. [PubMed: 21341261]
18. Chen ZJ, Sun L. J Nonproteolytic functions of ubiquitin in cell signaling. Mol. Cell. 2009; 33:275–286. [PubMed: 19217402]
19. Lu TT, et al. Dimerization and ubiquitin mediated recruitment of A20, a complex deubiquitinating enzyme. Immunity. 2013; 38:896–905. [PubMed: 23602765]
20. Lin SC, et al. Molecular basis for the unique deubiquitinating activity of the NF-kappaB inhibitor A20. J. Mol. Biol. 2008; 376:526–540. [PubMed: 18164316]
21. Shembade N, Ma A, Harhaj EW. Inhibition of NF-kappaB signaling by A20 through disruption of ubiquitin enzyme complexes. Science. 2010; 327:1135–1139. [PubMed: 20185725]
22. Bosanac I, et al. Ubiquitin binding to A20 ZnF4 is required for modulation of NF-κB signaling. Mol. Cell. 2010; 40:548–557. [PubMed: 21095585]
23. Skaug B, et al. Direct, noncatalytic mechanism of IKK inhibition by A20. Mol. Cell. 2011; 44:559–71. [PubMed: 22099304]
24. Tokunaga F, et al. Specific recognition of linear polyubiquitin by A20 zinc finger 7 is involved in NF-κB regulation. EMBO J. 2012; 31:3856–3870. [PubMed: 23032187]

25. Verhelst K, et al. A20 inhibits LUBAC-mediated NF-kB activation by linear polyubiquitin chains via its zinc finger 7. EMBO J. 2012; 31:3845–3855. [PubMed: 23032186]
26. Beyaert R, Heyninck K, Van Huffel S. A20 and A20 binding proteins as cellular inhibitors of NF-kB dependent gene expression and apoptosis. Biochem. Pharm. 2000; 60:1143–1151. [PubMed: 11007952]
27. Ch'en IL, Tsau JS, Molkentin JD, Komatsu M, Hedrick SM. Mechanisms of necroptosis in T cells. J. Exp. Med. 2011; 208:633–641. [PubMed: 21402742]
28. Osborn SL, et al. Fas-associated death domain (FADD) is a negative regulator of T-cell receptor mediated necroptosis. Proc. Natl. Acad. Sci. USA. 2010; 107:13034–13039. [PubMed: 20615958]
29. He S, et al. Receptor interacting protein kinase 3 determines cellular necroptotic responses to TNFa. Cell. 2009; 137:1100–1111. [PubMed: 19524512]
30. Cho Y, et al. Phosphorylation-driven assembly of the RIPK1-RIPK3 complex regulates programmed necrosis and virus-induced inflammation. Cell. 2009; 137:1112–1123. [PubMed: 19524513]
31. Li J, et al. The RIP1/RIP3 necrosome forms a functional amyloid signaling complex required for programmed necrosis. Cell. 2012; 150:339–350. [PubMed: 22817896]
32. Zamvil SS, Steinman L. The T lymphocyte in experimental allergic encephalomyelitis. Ann. Rev. Immunol. 1990; 8:579–621. [PubMed: 2188675]
33. Cua DJ, et al. Interleukin-23 rather than interleukin-12 is the critical cytokine for autoimmune inflammation of the brain. Nature. 2003; 421:744–748. [PubMed: 12610626]
34. Linkermann A, Green DR. Necroptosis. N. Engl. J. Med. 2014; 370:455–465. [PubMed: 24476434]
35. Udeshi ND, Mertins P, Svinkina T, Carr SA. Large-scale identification of ubiquitination sites by mass spectrometry. Nat. Prot. 2013; 8:1950–1960.
36. Vanlangenakker N, et al. TNF-induced necroptosis in L929 cells is tightly regulated by multiple TNFR1 complex I and II members. Cell Death Dis. 2011; 2:e230. [PubMed: 22089168]
37. Duong B, et al. A20 restricts ubiquitination of pro-interleukin-1β protein complexes and suppresses NLRP3 inflammasome activity. Immunity. 2015; 42:55–67. [PubMed: 25607459]
38. Opipari AW, Hu HM, Yabkowitz R, Dixit VM. The A20 zinc finger protein protects cells from tumor necrosis factor cytotoxicity. J. Biol. Chem. 1992; 267:12424–12427. [PubMed: 1618749]
39. Welz, et al. FADD prevents RIPK3-mediated epithelial cell necrosis and chronic intestinal inflammation. Nature. 2011; 477:330–334. [PubMed: 21804564]
40. Bates JS, et al. Meta-analysis and imputation identifies a 109 kb risk haplotype spanning TNFAIP3 associated with lupus nephritis and hematologic manifestations. Genes Immun. 2009; 10:470–477. [PubMed: 19387456]
41. Jiang X, et al. Expression of tumor necrosis factor alpha-induced protein 3 mRNA in peripheral blood mononuclear cells negatively correlates with disease severity in psoriasis vulgaris. Clin. Vaccine Immunol. 2012; 19:1938–1942. [PubMed: 23054742]
42. Kelly C, et al. Expression of the inflammatory regulator A20 correlates with lung function in patients with cystic fibrosis. J. Cyst. Fibros. 2013; 12:411–415. [PubMed: 23164641]
43. Kaiser WJ, et al. RIPK3 mediates the embryonic lethality of caspase-8-deficient mice. Nature. 2011; 471:368–372. [PubMed: 21368762]
44. Oberst A, et al. Catalytic activity of the caspase-8-FLIP(L) complex inhibits RIPK3-dependent necrosis. Nature. 2011; 471:363–367. [PubMed: 21368763]
45. Zhang H, et al. Functional complementation between FADD and RIPK1 in embryos and lymphocytes. Nature. 2011; 471:373–376. [PubMed: 21368761]
46. O'Donnell MA, et al. Caspase 8 inhibits programmed necrosis by processing CYLD. Nat. Cell Biol. 2011; 13:1437–1442. [PubMed: 22037414]
47. Moquin DM, et al. CYLD deubiquitinates RIP1 in the TNFα-induced necrosome to facilitate kinase activation and programmed necrosis. PLoS One. 2013; 8:E76841. [PubMed: 24098568]
48. Bertrand MJ, et al. Cellular inhibitors of apoptosis cIAP1 and cIAP2 are required for innate immunity signaling by the pattern recognition receptors NOD1 and NOD2. Immunity. 2009; 30:789–801. [PubMed: 19464198]

49. Bertrand MJ, et al. cIAP1 and cIAP2 facilitate cancer cell survival by functioning as E3 ligases that promote RIPK1 ubiquitination. Mol. Cell. 2008; 30:689–700. [PubMed: 18570872]
50. McComb S, et al. cIAP1 and cIAP2 limit macrophage necroptosis by inhibiting Rip1 and Rip3 activation. Cell Death Differ. 2012; 19:1791–1801. [PubMed: 22576661]
51. Sun L, et al. Mixed lineage kinase domain-like protein mediates necrosis signaling downstream of RIPK3 kinase. Cell. 2012; 148:213–227. [PubMed: 22265413]
52. Xie T, et al. Structural insights into RIPK3-mediated necroptotic signaling. Cell Rep. 2013; 5:70–78. [PubMed: 24095729]
53. Molnarfi N, et al. MHC class II-dependent B cell APC function is required for induction of CNS autoimmunity independent of myelin-specific antibodies. J. Exp. Med. 2013; 210:2921–2937. [PubMed: 24323356]

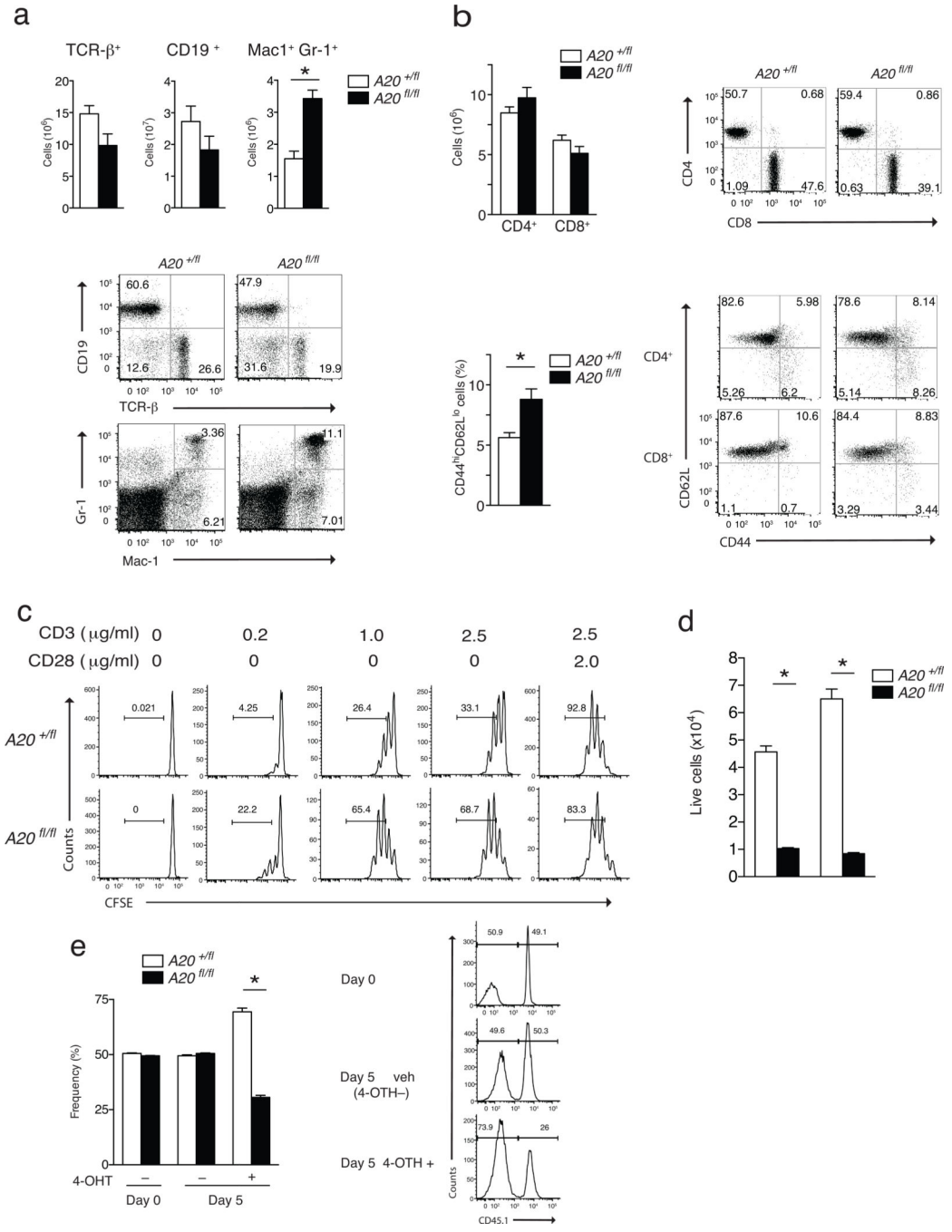

Figure 1. A20 supports T cell expansion

(**a**) FACS analyses of splenocytes from unperturbed A20$^{fl/fl}$ CD4-Cre (fl/fl) and control A20$^{+/fl}$ CD4-Cre (+/fl) mice. Quantitation of T (TCR-β^{+}), B (CD19^{+}), and myeloid (Mac-1^{+}, Gr-1^{+}) cell numbers are shown above; representative FACS plots are shown below. (b) FACS analyses of lymph node T cells from unperturbed A20$^{fl/fl}$ CD4-Cre (fl/fl) and control A20$^{+/fl}$ CD4-Cre (+/fl) mice. Quantitation of CD4^{+} and CD8^{+} T cell numbers and percentages of CD4 T cells expressing CD44^{high}CD62^{low} are shown at left; representative FACS plots shown at right. * indicates $p < 0.05$ by Student's T test; error bars

indicate standard deviations; n = 4 and 6 pairs of mice from 2 independent experiments for (a) and (b). (c) Representative FACS data showing CFSE dilution of naïve $CD4^+$ T cells of the indicated genotypes after stimulation with the indicated doses of agonist anti-CD3 (2.5 μg/ml and anti-CD28 (2.0 μg/ml) antibodies in vitro for three days. Numbers in each plot indicate percentages of cells that have diluted CFSE (i.e., divided). n = 2 pairs of mice, 2 independent experiments. (d) Live cell numbers of TCR activated naïve $CD4^+$ T cells from mixed cultures of $A20^{fl/fl}$ CD4-Cre (solid columns) and $A20^{+/fl}$ CD4-Cre (open columns) $CD4^+$ T cells. Numbers of live (DAPI negative) $CD4^+$ T cells of the indicated genotypes 48 and 72 hrs after in vitro stimulation with anti-CD3 and anti-CD28 antibodies as in (c) above. * indicates $p < 0.05$ by ANOVA; error bars indicate standard deviations; n = 3 pairs of mice, 5 independent experiments. (e) Reduced survival of $CD4^+$ T cells acutely rendered A20 deficient. Naïve $CD4^+$ T cells were purified from CD45 congenic $A20^{fl/fl}$ ROSA/ER-Cre and $A20^{+/fl}$ ROSA/ER-Cre mice, mixed, and treated with 4-OH-tamoxifen in the indicated samples during stimulation with anti-CD3 and anti-CD28 antibodies. Deletion of A20 protein from T cells was confirmed by immunoblotting (data not shown). The percentages of live $CD4^+$ T cell numbers from each of the two genotypes in each sample are measured (cell %) on the indicated days. Means and standard deviations are indicated. * indicates $p < 0.05$ between genotypes of mice. Representative histograms of CD45.1 expression on DAPI negative (live) cells are shown at right. Numbers within each histogram show the percentage of $CD45.1^+$ ($A2^{flLfl}$) and CD45.1 ($A20^{+/fl}$) cells within each sample. n = 2 pairs of mice, 2 independent experiments

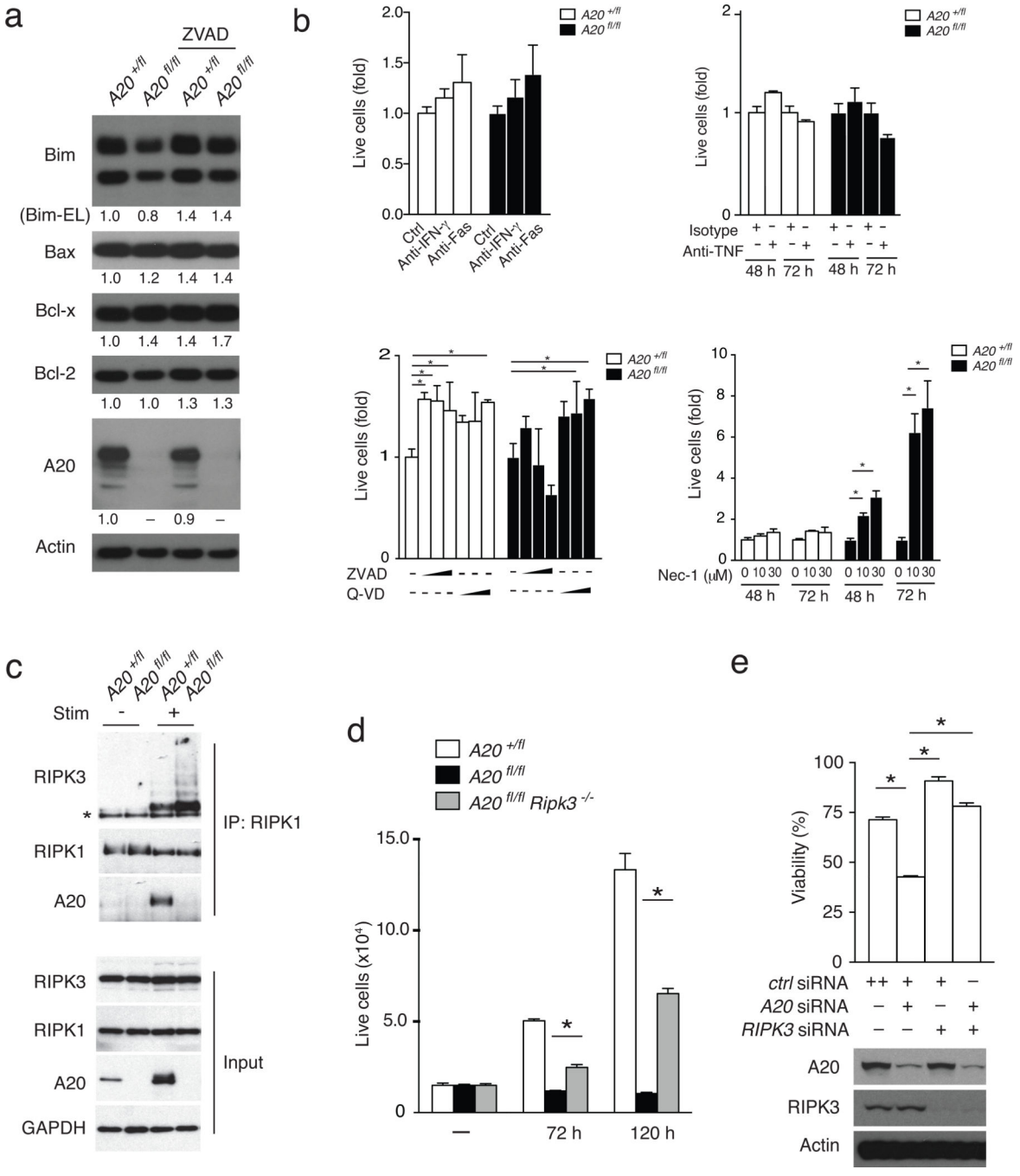

Figure 2. A20 inhibits T cell necroptosis

(a) Immunoblotting analyses of indicated survival proteins in TCR stimulated CD4^{+} T cells 13 hours after stimulation. Quantitation of immunoblots normalized to actin are shown below each blot. Actin and A20 protein levels are shown below as controls. Data are representative of 3 experiments using cells from 2 pairs of mice each. (b) Nec-1 sensitive death of A20$^{fl/fl}$ CD4-Cre T cells. Congenically marked A20$^{fl/fl}$ and A20$^{+/fl}$ T cells were co-cultured for 3 days with TCR stimulation in the presence of the indicated inhibitory antibodies or small molecules. In each graph, the numbers of live cells at each condition

were normalized to the numbers of cells of the same genotype obtained without blocking antibody or inhibitor. In lower left graph, ZVAD was used at 0, 10, 50 and 100 μM; and QVAD was used at 0, 20, and 40 μM for each genotype. Bars indicate standard deviations; * indicates $p < 0.05$ by 2-way ANOVA; n = 2 experiments using cells from 2 pairs of mice each. (c) Enhanced RIPK1-RIPK3 complexes in $A20^{fl/fl}$ CD4-Cre T cells. Immunoblotting analyses of RIPK1 associated proteins in $A20^{fl/fl}$ and $A2^{flL/+}$ CD4-Cre T cells before (−) and eight hours after (+) TCR stimulation. Note induction of A20 by TCR stimulation in $A20^{+/fl}$ CD4-Cre T cells. Note induction of RIPK1 associated RIPK3 in both $A20^{fl/fl}$ and $A20^{+/fl}$ CD4-Cre T cells, with greater RIPK3 recruitment in $A20^{fl/fl}$ CD4-Cre T cells. Data are representative of 3 experiments. (d) Rescue of survival of $A20^{fl/fl}$ CD4-Cre T cells by RIPK3 deficiency. Live cell numbers of $CD4^+$ T cells from indicated genotypes of mice at indicated time points after stimulation with anti-CD3, anti-CD28, plus ZVAD. Bars represent standard deviations; * indicates $p < 0.05$; n = 3 sets of mice from 2 experiments. (e) Rescue of A20 deficient Jurkat I9.2 cells by RIPK3 deficiency. Caspase 8 deficient Jurkat I9.2 cells were transfected with the indicated combinations of siRNAs, and stimulated 72 hours later with TNF. The percentage of surviving cells compared to non-stimulated Jurkat I9.2 cells is shown. Immunoblots for A20, RIPK3 and actin on treated cells are shown below as controls. Bars indicate standard deviations; * indicates $p < 0.05$ by one way ANOVA; n = 2 experiments.

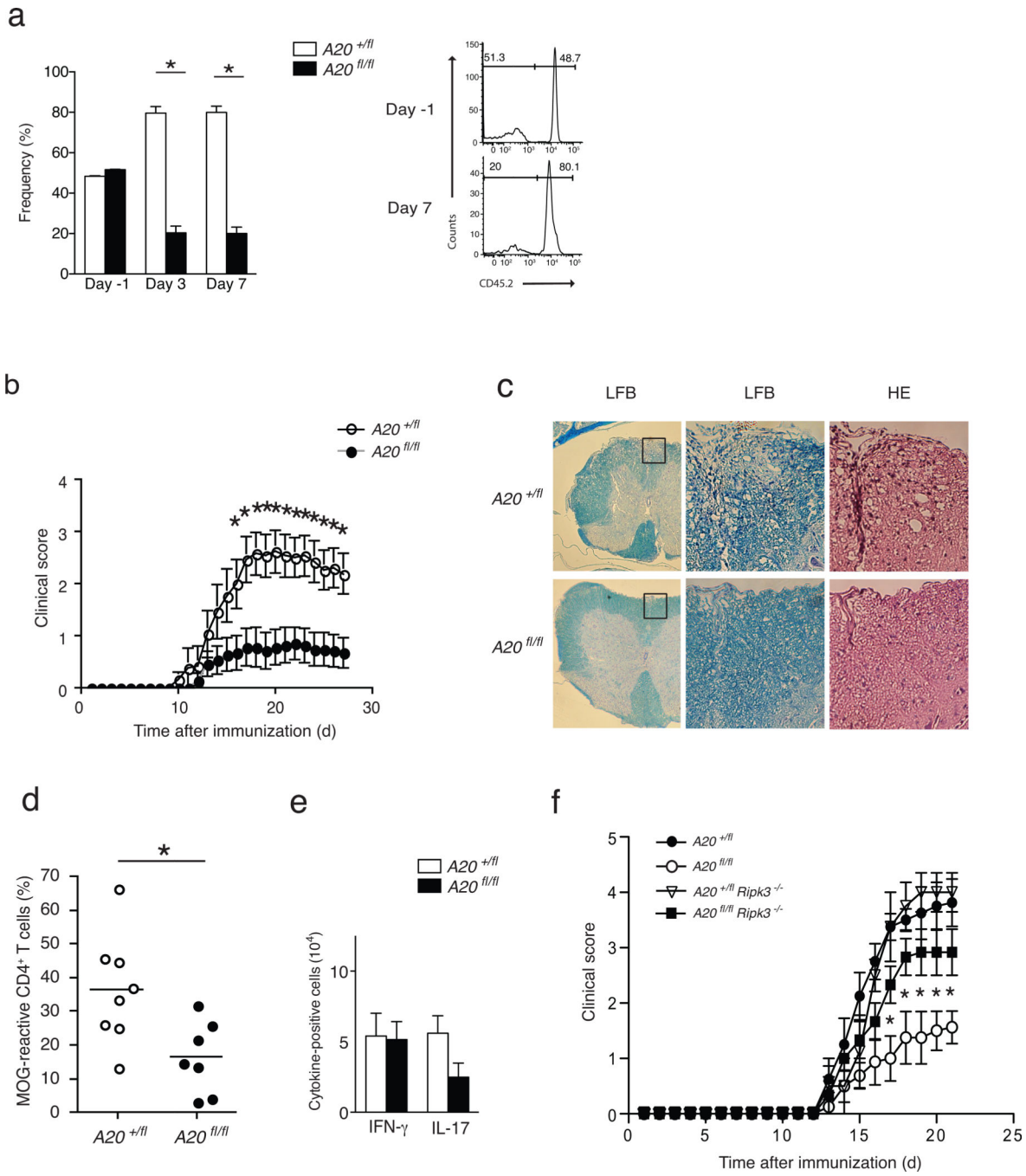

Figure 3. A20 supports antigen specific and autoimmune T cell responses in vivo

(a) Reduced in vivo expansion of $A20^{fl/fl}$ CD4-Cre OT-II $CD4^+$ T cells. FACS purified naïve ($CD4^+$ $CD62L^{Hi}$ CD25) $CD4^+$ OT-II cells from congenic $A20^{+/fl}$ CD4-cre CD45.1/45.2 and $A20^{FL/FL}$ CD4-cre CD45.1 mice were mixed 1:1, and co-transferred into congenic CD45.2 C57BL/6J recipients (Day −1). Mice were immunized with LPS plus OVA peptide 24 hours later (Day 0). The percentage of live OT-II $CD4^+$ T cells from each genotype on the indicated days is indicated. Each time point represents data from 3 mice. Representative histograms at right show CD45.2 expression after gating on $CD45.1^+$ (donor)

cells. Numbers within each histogram reflect the percentage of $CD45.1^+$ (donor) cells that are either CD45.2 ($A20^{fl/fl}$) or $CD45.2^+$ ($A20^{+/fl}$). Data analyzed by two-way ANOVA, error bars represent mean +/− SEM; n = 3 mice of each genotype from 2 independent expts. (b) Reduced EAE in $A20^{fl/fl}$ CD4-Cre mice. Serial EAE clinical scores of $A20^{fl/fl}$ CD4-Cre (fl/fl) and control $A20^{+/fl}$ CD4-Cre (+/fl) mice after immunization with MOG plus CFA. Means and standard errors are indicated. * indicates $p < 0.05$ between genotypes of mice on the indicated days. Data were obtained from 14 $A20^{fl/fl}$ CD4-Cre and 13 control mice and represent 2 experiments. (c) Representative histopathological analyses of spinal cord sections from the indicated mice 30 days after immunization. Luxol fast blue stains (LFB) highlighting myelin content of spinal cord sections from indicated mice (low magnification, left panels). Higher magnification images of boxed areas showing LFB and hematoxylin and eosin (HE) stains of tissue with infiltrating lymphocytes (right panels). Data are representative of 6 sets of mice and 2 experiments. (d) FACS quantitation of MOG reactive LN $CD4^+$ T cells. Nine days after immunization with MOG, LN T cells from the indicated mice were harvested, labeled with CFSE, and re-stimulated with MOG for 3 days in vitro. The percentage of CFSE labeled T cells in diluted versus non-diluted peaks after 3 days is indicated. Horizontal lines indicate means. * indicates $p < 0.05$ by Students T test; n = 7 and 8 mice from 2 experiments. (e) Reduced T_H17 cells from $A20^{fl/fl}$ CD4-Cre mice during EAE. Lymph node $CD4^+$ T cells from MOG immunized mice of the indicated genotypes were harvested, restimulated in vitro, and quantitated by flow cytometry for intracellular expression of the indicated cytokines. The numbers of $CD4^+$ T cells expressing IFNγ and IL17 are displayed. Data analyzed by Student's T test; horizontal lines indicate means +/− SEMs; n = 3 sets of mice in 2 experiments. (f) RIPK3 deficiency restores EAE susceptibility of $A20^{fl/fl}$ CD4-Cre mice. Serial EAE clinical scores of RAG-$1^{-/-}$ mice bearing T cells of the indicated genotypes after immunization with MOG. Means and standard errors are indicated. Note that $A20^{fl/fl}$ CD4-Cre $RIPK3^{-/-}$ T cells (filled squares) cause significantly more severe EAE symptoms than $A20^{fl/fl}$ CD4-Cre T cells (open circles). Data analyzed by two way ANOVA; $p < 0.05$ between $A20^{FL/FL}$ CD4-Cre and $A20^{fl/fl}$ CD4-Cre $RIPK3^{-/-}$ T cells for all days after day 17; n = 5 mice of each genotype in 2 experiments.

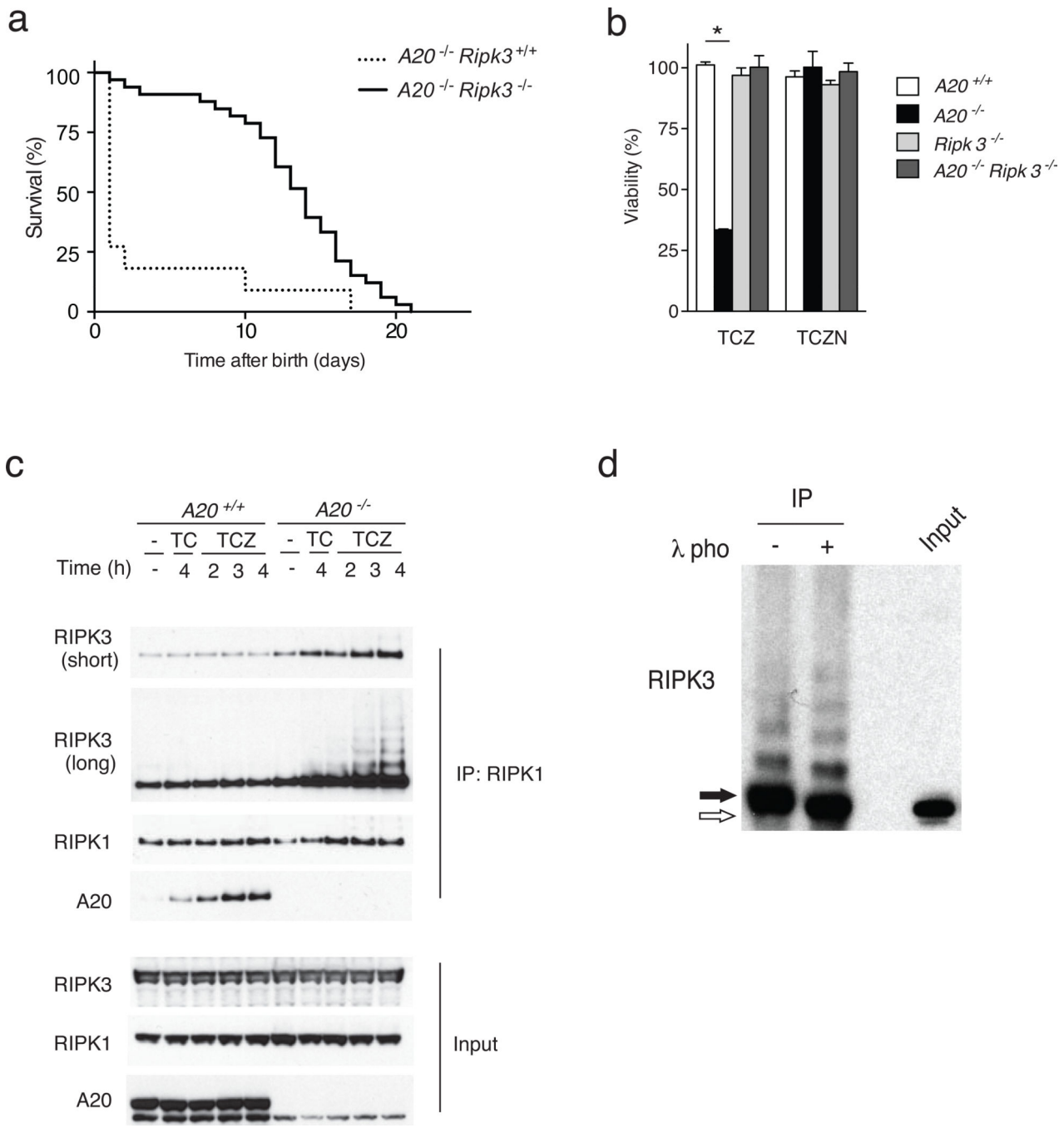

Figure 4. A20 inhibits RIPK1-RIPK3 complex formation

(a) Spontaneous survival of *A20*$^{ko2/ko2}$ *Ripk3*$^{-/-}$ (*A20*$^{-/-}$ *Ripk3*$^{-/-}$, solid line) and *A20*$^{ko2/ko2}$ *Ripk3*$^{+/+}$ (*A20*$^{-/-}$ *Ripk3*$^{+/+}$, dotted line) littermate mice in days after birth. Data represent 33 *A20*$^{-/-}$ *Ripk3*$^{-/-}$ mice and 16 *A20*$^{-/-}$ *Ripk3*$^{+/+}$ mice, with each step representing death of one mouse. The mean survival *A20*$^{-/-}$ *Ripk3*$^{-/-}$ mice was 14 days, while the mean survival of *A20*$^{-/-}$ *Ripk3*$^{+/+}$ mice was less than 1 day, with enhanced survival of *A20*$^{-/-}$ *Ripk3*$^{-/-}$ mice over *A20*$^{-/-}$ *Ripk3*$^{+/+}$ mice statistically significant at $p < 0.0001$ by Logrank test. (b) Survival of MEFs of the indicated genotypes 4 hours after stimulation with either TNF,

CHX, and ZVAD (TCZ), or TNF, CHX, ZVAD, and Nec1 (TCZN). Note that Nec1 rescues cell death of *A20*$^{ko2/ko2}$ *Ripk3* cells, as does RIPK3 deficiency. Bars indicate the proportion of live cells relative to unstimulated cells of the same genotype. * indicates $p < 0.05$; n = . (c) RIPK1-RIPK3 complexes in stimulated MEFs. RIPK3 and A20 expression in anti-RIPK1 IPs from *A20*$^{-/-}$ or wild- type (WT, or *A20*$^{+/+}$) MEFs stimulated with the indicated agents for the indicated time periods. Total cell lysate protein levels (input) are shown below as controls. Note the increased RIPK1 associated RIPK3 in *A20*$^{-/-}$ cells, with laddered, higher molecular weight forms of RIPK3. Note also the A20 recruitment to RIPK1 in WT cells. (d) Phosphorylation of RIPK1 associated RIPK3. *A20*$^{-/-}$ MEFs were stimulated as in (c) above, after which lysates were immunoprecipitated with anti-RIPK1, treated with lambda phosphatase (+) or control buffer (−), and analyzed by immunoblotting for RIPK3. Whole cell lysate at right (input) shows size of native RIPK3 protein as control. Note that RIPK1-associated RIPK3 is almost entirely phosphatase sensitive in stimulated *A20*$^{-/-}$ cells undergoing necroptosis.

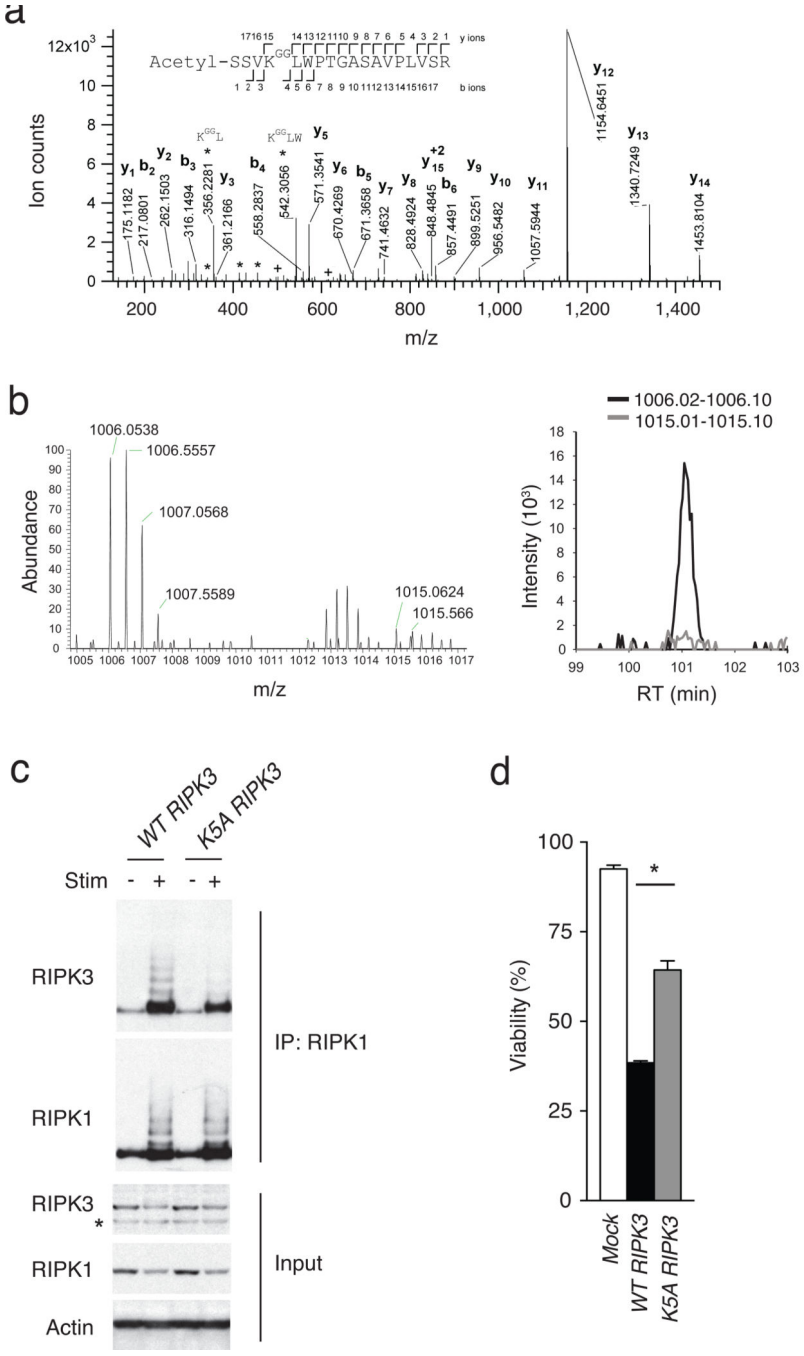

Figure 5. RIPK3 ubiquitination supports RIPK1-RIPK3 complexes and necroptosis

(a) Site specific ubiquitination of RIPK3. *A20*$^{-/-}$ MEFs were stimulated with TNF, CHX and ZVAD, and lysed after 4 hours. Lysates were immunoprecipitated with anti-gly-gly antibody, after which immunoprecipitates were analyzed by nanoflow-UPLC-HCD-MSMS. A HCD tandem mass spectrum obtained from a precursor ion with m/z value 1006.0525^{+2} from *A20*$^{-/-}$ cells undergoing necroptosis is shown. A data base search showed the spectra to identify the peptide spanning amino acids 2 to 19 of RIPK3, acetylated in the N terminus and carrying a di-glycine remnant on K5 (theoretical monoisotopic m/z= 1006.0522^{+2}).

Sequence ions are labeled in the figure, and indicated with marks over (C-terminal ions) and below (N-terminal ions) the sequence of the peptide. Prominent ions corresponding to internal fragments are labeled (*). Ions labeled (+) show fragments with masses 501.2667 and 614.3508, corresponding to ions b4 and b5 undergoing a second fragmentation, with a loss of 57.02146 mass units, corresponding to the terminal glycine on the ε-amino of RIPK3 K5. (b) SILAC based mass spectrometric quantitation of RIPK3 ubiquitination. Heavy (*A20*$^{+/+}$) and light (*A20*$^{-/-}$) isotope labeled MEFs were stimulated to undergo necroptosis, after which cell lysates were mixed and then analysed by ubiscan assisted mass spectrometry as in (a). The di-glycine remnant of RIPK3 K5 from light isotope labeled cells (*A20*$^{-/-}$ cells) was again identified at m/z = 1006, while the heavy isotope labeled cells (*A20*$^{+/+}$ cells) contained the RIPK3 K5 peptide at m/z = 1015 (spectra on left). The relative abundance of these two forms of the ubiquitinated K5 peptide is displayed in the histogram at right. (c) K5 ubiquitination supports RIPK1-RIPK3 complexes. WT or mutant K5A RIPK3 expression constructs were transduced into *A20*$^{-/-}$ RIPK3$^{-/-}$ MEFs using a GFP-expressing lentivirus, after which cells were FACS-sorted to obtain pure populations of transduced (GFP^{+}) cells. Cells were then stimulated for four hours, lysed and analysed for RIPK1-associated RIPK3 expression by immunoblotting. “+” indicates treatment with TNF, CHX, and ZVAD; “-” indicates media control. RIPK1 immunoblot of RIPK1 IP is shown below RIPK3 immunoblot as control for IP; immunoblots for RIPK3, RIPK1, and actin on whole cell lysates are shown below as controls. * indicates non-specific band below specific RIPK3 band. (d) K5 ubiquitination supports necroptosis. *A20*$^{-/-}$ *Ripk3*$^{-/-}$ MEFs complemented with RIPK3 constructs in (c) above analyzed for sensitivity to necroptosis. Survival of MEFs expressing the indicated forms of RIPK3 is shown relative to unstimulated cells. Bars indicate standard deviation. * indicates $p < 0.05$ when compared with cells expressing WT RIPK3.

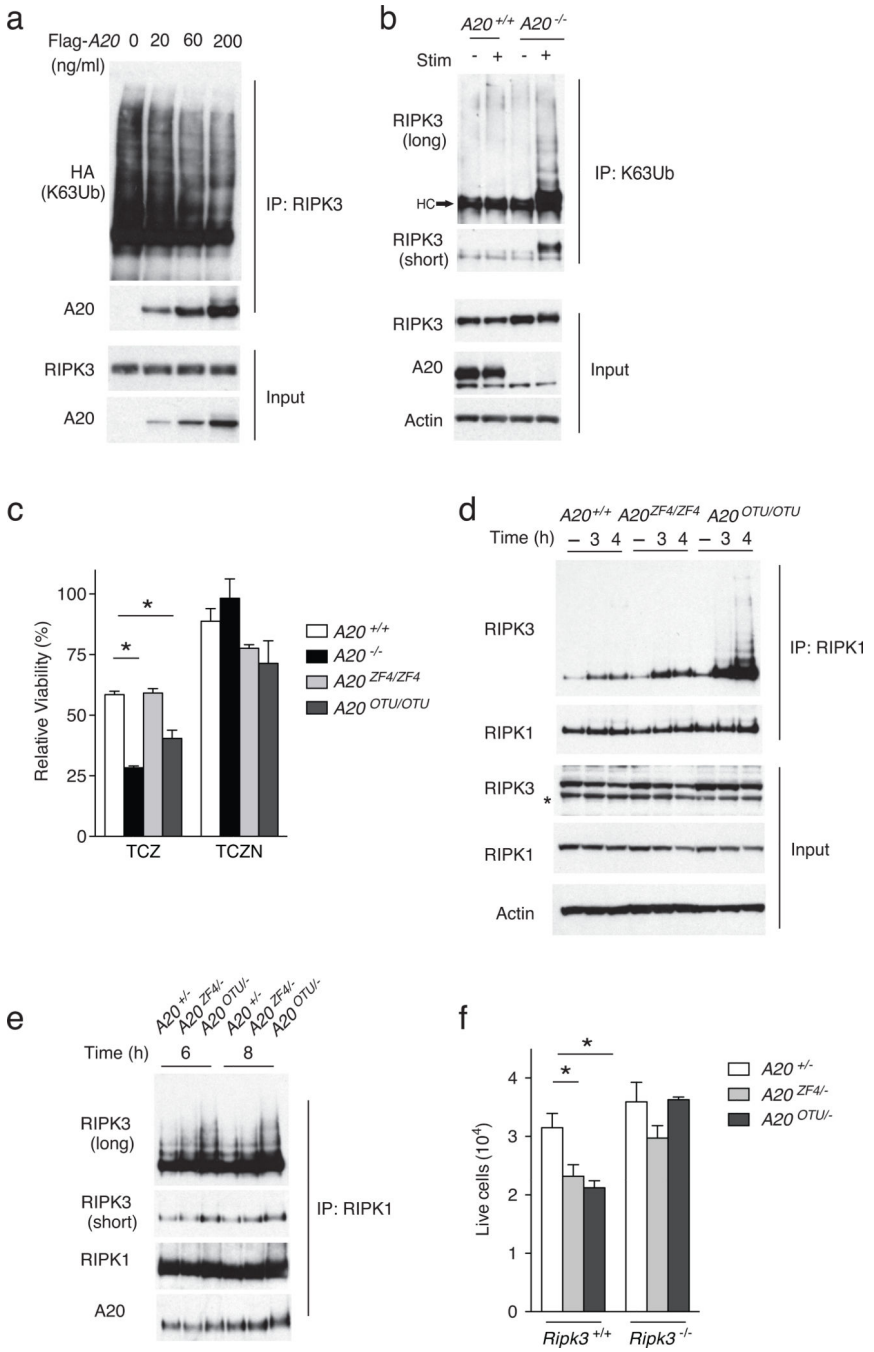

Figure 6. A20 utilizes its C103 motif to inhibit RIPK1-RIPK3 complexes

(a) A20 mediated deubiquitination of K63-ubiquitinated RIPK3. 293T cells were transfected with plasmids expressing RIPK3, HA-K63-Ub (HA-tagged ubiquitin in which all ubiquitin lysines except K63 were mutated to arginine), and FLAG-A20, immunoprecipitated with anti-RIPK3, and immunoblotted for HA (K63-ubiquitin) and A20. Immunoblots of whole cell lysates for RIPK3 and A20 are shown below as controls. (b) K63-ubiquitination of RIPK3 in $A20^{-/-}$ cells. $A20^{+/+}$ and $A20^{-/-}$ MEFs were stimulated with TNF, CHX and ZVAD (TCZ) ("stim +"), and lysed under denaturing conditions (6M urea). Lysates were

diluted, imunoprecipitated with anti-K63 ubiquitin antibody, and analyzed for RIPK3 expression. Short exposure of RIPK3 immunoblot shown to demonstrate increased and phosphorylated RIPK3; long exposure shown to demonstrate increased K63-ubiquitination of RIPK3. Immunoblots of whole cell lysates for RIPK3, A20 and actin are shown on whole cell lysates below as controls. Note the increased K63-ubiquitinated RIPK3 in stimulated *A20*$^{-/-}$ cells. Data are representative of 3 independent experiments. (c) Cell survival of the indicated genotypes of MEFs after stimulation with TNF, CHX and ZVAD (TCZ) or TNF, CHX, ZVAD and Nec1 (TCZN) for five hours. Bars indicate standard deviation. * indicates $p < 0.05$ by ANOVA when compared with WT cells. (d) RIPK1-RIPK3 complexes in indicated genotypres of MEFs treated with TCZ as in (c) above. RIPK1 expression in IPs is shown as control. RIPK1, RIPK3 and actin expression in whole cell lysates shown below as controls. (e) RIPK1-RIPK3 complexes in indicated genotypes of T cells stimulated with anti-CD3, anti-CD28, and ZVAD for the indicated time periods. Short and long exposures of RIPK1 associated RIPK3 shown; RIPK1 and A20 expression in RIPK1 IPs are shown as controls. (f) Live cell numbers of indicated genotypes of T cells after TCR stimulation as in (e) for 72 hours. Bars indicate standard deviation. * indicates $p < 0.05$ when compared with WT cells. Data are representative of 3 independent experiments.